LA-UR- 98-2711

Approved for public release; distribution is unlimited.

Title: Molecular Dynamics Simulations of Dipolar Dusty Plasmas

CONF-980456--

Author(s): J. E. Hammerberg, XNH
B. L. Holian, T-12
M. S. Murillo, XPA
D. Winske, XPA

Submitted to: Proceedings of the 7th Workshop on Dusty Plasmas

Los Alamos
NATIONAL LABORATORY

DISCLAIMER

Molecular Dynamics Simulations of Dipolar Dusty Plasmas

J. E. Hammerberg, B. L. Holian, M. S. Murillo and D. Winske

Los Alamos National Laboratory
Los Alamos, NM 87545

Abstract. We use molecular dynamics (MD) simulation methods to investigate dusty plasma crystal structure in an external potential, with the grains subject to both a spherically symmetric Debye-Hückel potential and a cylindrically symmetric dipole interaction. The dipole contribution models the experimentally important effects of ion flow or intrinsic grain polarization. We find that the addition of a small dipole term changes the crystal structure from bct to one in which the grains are aligned vertically, consistent with experiments as well as recent theoretical calculations.

Introduction

Crystalline structures have been commonly produced in dusty plasmas in recent years (1-4), some time after they were predicted (5). The experiments are relatively simple, requiring a small rf discharge plasma, a way to introduce the grains into the system, as well as a laser scattering system and a video camera to observe the individual grains. In the plasma, the grains become charged and reside in electrostatic traps at the edge of the sheath above the lower electrode (6), where the electrostatic repulsion from the electrode balances gravity. For a particular range of gas pressure and rf power, the grains can form into a regular array, which is typically 2-20 layers thick and extends to cm size in the transverse directions. The grains are usually 5-10 μm in diameter and acquire a negative charge that is on the order of 10^4 electronic charges. The intergrain spacing is several hundred microns, which is roughly the electron Debye length in an (argon) plasma of electron number density $n_e \sim 10^9$ cm^{-3} and temperature $T_e \sim 2$ eV. In some plasma crystals, either fcc or bcc structures have been observed (2), while in other experiments, the grains in each layer seem to be aligned vertically (4).

A number of numerical simulations of crystal formation have been performed using molecular dynamics (7-11). In these calculations the charged dust grains are assumed to interact via a screened Coulomb potential, similar to that used in the study of strongly coupled Coulomb systems (12). However, the dust crystal experiments add several complications not found in the usual theoretical studies. First, there is cooling due to the interaction of the grains with the background neutrals. Usually this is treated

by means of a thermostat in the simulations, although it is possible to include the dust-neutral interactions directly (7). Second, the confining effect of the electrostatic trap also needs to be taken into account. This potential includes the effect of gravity as well as the time-averaged electric field in the sheath region above the electrode. It has been modeled as a simple symmetric parabolic potential (10) or as an asymmetric Morse potential (11). Simulations with this simple model result in structures that are close-packed layers with dislocations (11).

On the other hand, experiments often exhibit a striking tendency for one-dimensional order in the direction normal to the electrode (4). For example, simple hexagonal patterns are observed with one axis oriented normal to the electrode. Since deviations from sphericity in the interaction potential can change the energy landscape in such a way that more distorted arrangements of dust grains may be the lower lying structures, this suggests that other physical effects in the experiments need to be included in the computational model. One such effect is the flow of ions in the sheath that is directed toward the electrode. This can be included by adding either flow in the fluid equations for the background plasma (8-9) or an asymmetric potential around each grain to account for the flow (9). This asymmetric potential structure has been investigated theoretically (13) and has been studied in self-consistent particle simulations of electron and ion flow around a stationary dust grain (14).

A simple way to include these asymmetric effects in the simulations is to model them as dipole interactions. Because the dipole effect can be thought of as arising from the focusing of flowing ions behind a dust grain, the size of the force on neighboring grains due the dipole can be comparable to that due to the monopole force. In two-layer dust crystals, MD simulations have been used to estimate the strength of the dipole (15). Use of a dipole to describe the top layer only, leads to an asymmetric force between the two layers and interesting stability properties of this system. More generally, the dipole model can also take into account the intrinsic polarization of the grains interacting with the sheath electric field (16). Recently, Lee et al. (17) have included a dipole moment to calculate the energy of a dusty plasma crystal and obtain a phase diagram as a function of lattice spacing and the magnitude of the dipole contribution relative to the monopole force. For increasing dipole moment, they find non-close packed lattice structures that exhibit a linear chain structure along the axis of the dipole orientation.

In this paper, we present first results of molecular dynamics simulations that include a dipole moment and an improved model for the external potential. We find that the addition of a small dipole contribution allows the grains to align vertically and thus change the crystal structure from bct to other configurations. We thus determine the stability of the structures obtained by Lee et al. (17) in a dynamic context with a realistic external potential.

Simulation Model and Results

We assume the interaction between dust particles consists of two parts. The first part is due to the direct interaction between dust particles plus the induced interaction due to the dielectric polarizability of the plasma. This gives rise to a spherically symmetric Debye-Hückel potential

$$\phi_o(r) = \frac{e^{-r}}{r}, \tag{1}$$

where we normalize lengths to the electron Debye length, λ, and energy to Q^2/λ, where Q is the charge on the dust grain.

The second contribution is directional, which is due to an underlying cylindrical symmetry in the charge distribution about an external field direction, that we take to be in the z-direction. We model this by an effective dipole interaction

$$\phi_D(r,z) = \phi_1(r) - \phi_2(r) z^2, \tag{2}$$

where this contribution to the potential due to local charge non-sphericity is given by a spherically symmetric term, ϕ_1, and an axially symmetric term, $\phi_2 z^2$, which are of the form

$$\phi_1(r) = \phi_o(r)[1 + \frac{\mu(r)}{r}(1 + \frac{1}{r})], \tag{3}$$

$$\phi_2(r) = \frac{\mu(r)}{r^2}\phi_o(r)[1 + \frac{3}{r}(1 + \frac{1}{r})]. \tag{4}$$

The quantity μ is the square of the dipole moment. We take into account the fact that for small separations (which in a molecular dynamics simulation will occur if a potential of the form ϕ_2 is used with constant μ), the dipole approximation breaks down and the limiting interaction is strongly repulsive, by defining an effective r-dependent dipole moment

$$\mu(r) = \mu_o[1 - \exp(-\gamma r^4)], \tag{5}$$

where $\gamma = \ln(2) / (16\mu_o^2)$. This vanishes as $r \to 0$ and begins to decrease when the effective radii of the dipole distributions are in contact. The fourth power ensures that $\phi \to \phi_o$ for small r.

We also include an effective external trapping potential, which is given by the sum of an electrostatic term to model the electric field in the sheath that pushes the negatively charged grains upward away from the electrode and a gravitational term that pushes them downward, of the form

$$\phi_X(z) = b[\frac{1}{\alpha}e^{-\alpha z} + z]. \tag{6}$$

This form is appropriate only for fairly large dust grains (≥ 5 μm), since the ion drag force is ignored. In the calculations here we assume a grain radius of a = 5 μm and an electric field of 60 V/cm. In our units, assuming $Q = -10^4 |e|$ and $\lambda = 300$ μm, we have b=3.6 and $\alpha = 0.06$.

In the MD simulations we solve the equations of motion for dust grains of mass M = 1.0 ng for $\Gamma_\lambda = Q^2/\lambda k_B T = 333$. We initialize the calculations with a cube of 10^3 particles with unit spacing and equilibrate this system at $\Gamma_\lambda = 10$ for $10t_o$ ($t_o = [M\lambda^3/Q^2]^{1/2}$ corresponding to about 0.05 sec for our parameters) with no external potential imposed. At this high temperature the system forms a uniform fluid state. At 10 t_o, the system size is increased in the z-direction by a factor of three. The system is then rapidly quenched in the external potential (6) to $\Gamma_\lambda = 333$. The system expands along the z-axis and reaches a steady state that shows long-range order. In all cases, the boundaries at $x = \pm 5$ and $y = \pm 5$ are periodic. The z boundaries at ± 15 are free in the quenched state, but the confined system never reaches these boundaries.

In Figs. 1 and 2 we present results for one representative case, $\mu_o = 0.025$. Figure 1 shows the view of the system along the x-axis for times 10 t_o, 100 t_o, 200 t_o, 300 t_o, 400 t_o, 500 t_o, 600 t_o, 700 t_o, and 800 t_o. The time sequence is vertical, from left to right. The initial frame shows the system as it has equilibrated in the smaller system ($-5 < z < 5$). Thereafter, the system size is extended, the external potential is applied, and the grains expand in z. By $t = 200t_o$, some vertical alignment has begun in the center of the system. The alignment increases with time, so that by the end of the run it has extended nearly throughout the entire system. The final state is an R2 structure, consisting of rectangular lattices shifted to the body center on successive planes in the z-direction. To see this more clearly, we show in Fig. 2 the two central planes. The left column shows the upper and lower planes, respectively. The dust aligns into

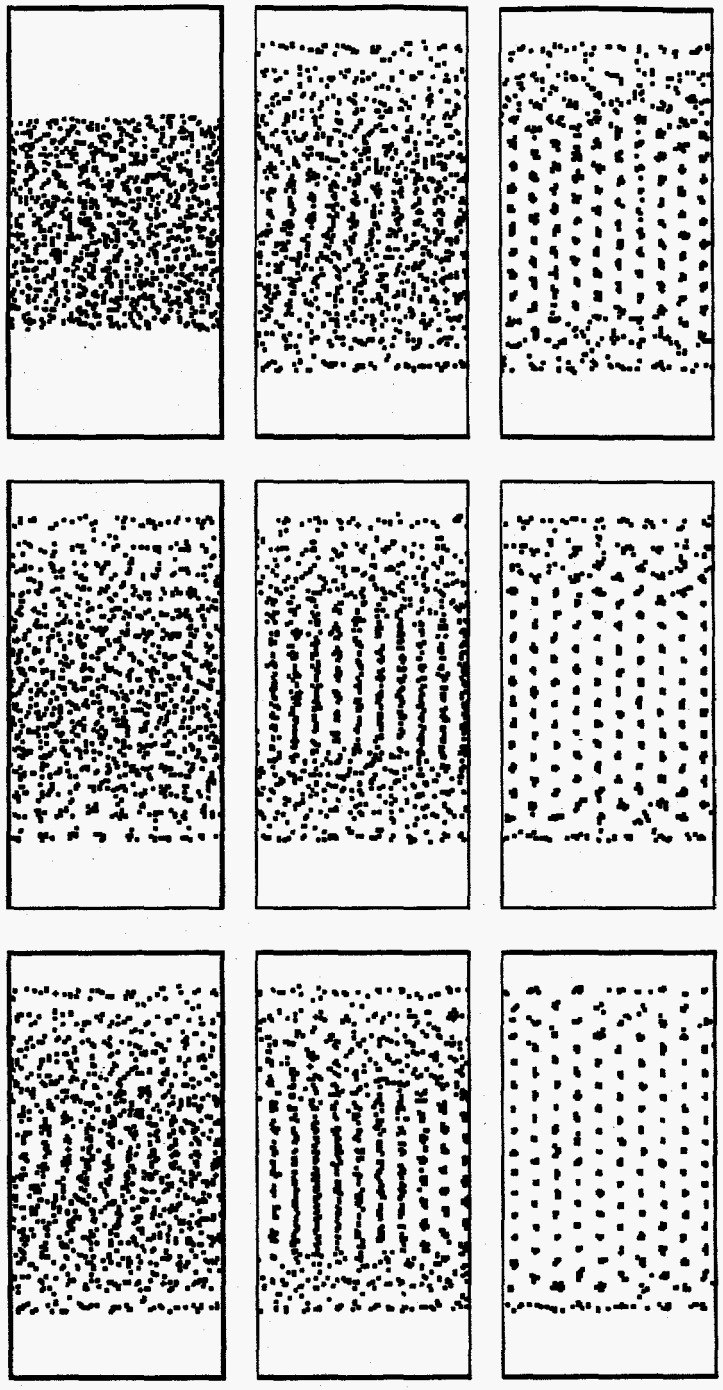

FIGURE 1. Evolution of the system with dipole strength $\mu_o = 0.025$, showing vertical alignment in time. The time sequence is from top to bottom, left to right, with t = 10 t_o, 100 t_o, 200 t_o, 300 t_o, 400 t_o, 500 t_o, 600 t_o, 700 t_o, and 800 t_o.

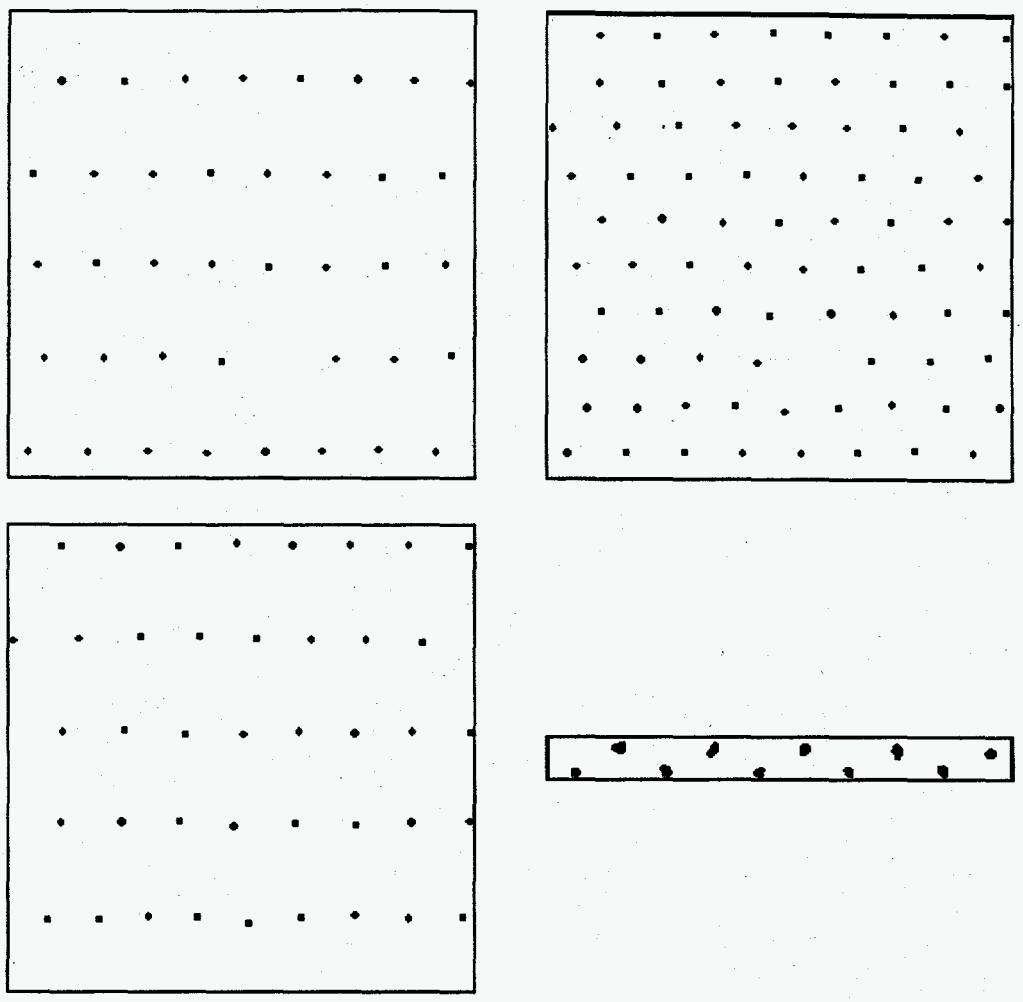

FIGURE 2. Left panels show dust alignment in two adjacent planes in the central region. The top right panel is their superposition; the bottom right panel is a side view.

rectangles, although the structures are evidently not perfect. The top plot in the right column is the composite image of these two planes that gives a hexagonal structure. The bottom plot at the right is the side view, showing the relative shift of these two planes.

We have carried out simulations for a range of values of μ_o: 0.0 0.01, 0.025, and 0.10. For $\mu_o = 0$, the system crystalizes in an bct(110) structure. As μ_o increases, the structure changes from Rh2 ($\mu_o = 0.01$) to R2 ($\mu_o = 0.025$) to T1 ($\mu_o = 0.1$), where we use the notation of Lee et al. (17). The Rh2 structure may also be described as a bct (110) lattice. The T1 structure is a simple hexagonal lattice. For higher values of μ_o, the dust arrangement becomes more disordered, as the edge of the trap is approached. There are also indications of phase coexistence of different structures, as one goes from the central region to the upper edge. All structures for nonzero μ_o are characterized by strong vertical alignment. However, these static images do not show, particularly in the $\mu_o = 0.1$ case, the considerable fluctuations in chain dynamics along the z-direction. The motion of these coherent chains is much larger than the displacements of the chains in the x and y directions.

Summary

We have investigated the dynamics of charged dust grains trapped in a plasma sheath and gravitational potential. We have included in the simulations both a Debye-Hückel central potential and a phenomenological dipolar interaction, which may have its origin in wake potentials or induced dipole moments in the charge distributions. The inclusion of the spherical symmetry breaking leads to ordered lattices characterized by significant linear coherence along the field direction (z-axis). For non-zero dipole moment, the ground state is no longer close-packed as was the case for $\mu_o = 0$. The structures correspond to the R2 and T1 structures predicted by Lee et al. (17) in their equilibrium analysis, but the dynamic structures are defective, exhibiting in-plane dislocations and relatively fluid motion of the vertical strings in the case of large μ_o. Whether these structures correspond in detail to the experimental structures is both a theoretical challenge in the proper calculation of the interaction potential and an experimental challenge in determining more of the microscopic parameters and structure of condensed dusty plasmas.

Acknowledgments

This work was supported by the Laboratory Directed Research and Development Program.

References

1. Chu, J. H., and I, L., *Phys. Rev. Lett.*, **72**, 4009-4012 (1994).
2. Thomas, H., Morfill, G. E., Demmel, V., Goree, J., Feuerbacher, B., and Mohlmann, D., *Phys. Rev. Lett.*, **73**, 652-655 (1994).
3. Melzer, A., Homann, A., and Piel, A., *Phys. Rev. E.*, **53**, 2757-2766 (1996).
4. Pieper, J. B., Goree, J., and Quinn, R. A., *J. Vac. Sci. Technol. A*, **14**, 519-524 (1996).
5. Ikezi, H., *Phys. Fluids*, **29**, 1764-1766 (1986).
6. Selwyn, G. S., Singh, J., and Bennett, R. S., *J. Vac. Sci. Technol. A*, **4**, 2758-2765 (1989).
7. Zheng, X. H., and Earnshaw, J. C., *Phys. Rev. Lett.*, **75**, 4214-4217 (1995).
8. Melandso, F., and Goree, J., *J. Vac. Sci. Technol. A*, **14**, 511-517, (1996).
9. Melandso, F., *Phys. Rev. E.*, **55**, 7495-7506 (1997).
10. Totsuji, H., Kishimoto, T., and Totsuji, C., *Phys. Rev. Lett.*, **78**, 3113-3116 (1997).
11. Hammerberg, J. E., Holian, B. L., Lapenta, G., Murillo, M. S., Shanahan, W. R., and Winske, D., MD "Simulations of dusty plasma crystal formation: Preliminary results," Proc. Intern. Conf. on Strongly Coupled Coulomb Systems, in press (1998).
12. Hammerberg, J. E., Holian, B. L., and Ravelo, R., *Phys. Rev. E.*, **50**, 1372-1375 (1994).
13. Ishihara, O., and Vladimirov, S. V., *Phys. Plasmas*, **4**, 69-74 (1997).
14. Lapenta, G., and Brackbill, J. U., *Phys. Rev. Lett.*, submitted (1998).
15. Schweigert, V. A., Schweigert, I. V., Melzer, A., Homann, A., and Piel, A., *Phys. Rev. E*, **54**, 4155-4166 (1996).
16. Mohideen, U., Rahman, H. U., Smith, M. A., Rosenberg, M., and Mendis, D. A., *Phys. Rev. Lett.*, **80**, in press (1998).
17. Lee, H. C., Chen, D. Y., and Rosenstein, B., *Phys. Rev. E.*, **56**, 4596-4607 (1997).